

## Synthesis and characterization of $\pi$ -conjugated peptide-based supramolecular materials\*

Brian D. Wall<sup>1</sup> and John D. Tovar<sup>1,2,‡</sup>

<sup>1</sup>*Department of Chemistry, Krieger School of Arts and Sciences, Johns Hopkins University, 3400 N. Charles St., Baltimore, MD 21218, USA;* <sup>2</sup>*Department of Materials Science and Engineering, Whiting School of Engineering, Johns Hopkins University, 3400 N. Charles St., Baltimore, MD 21218, USA*

**Abstract:** We describe the synthesis, characterization, and fabrication of bioelectronic materials derived from small oligopeptides containing  $\pi$ -conjugated subunits directly embedded into peptide backbones. The rapid incorporation of  $\pi$ -conjugated subunits directly into peptide backbones was accomplished through an on-resin dimerization procedure recently explored in our research. We investigated these peptides' abilities to self-assemble in aqueous environments into 1D nanostructures with intimate  $\pi$ - $\pi$  interactions. Finally, we discuss a simple processing method to develop aligned networks of 1D  $\pi$ -conjugated peptide nanostructures where the resulting electronic and photophysical properties are altered as a direct impact of the aligned  $\pi$ -conjugated network.

**Keywords:** biomaterials; chromophores;  $\pi$ -conjugated peptide nanostructures; nanomaterials; organic semiconductors; peptides; self-assembly.

### INTRODUCTION

Complex assemblies of molecular components have an ever-increasing role in the field of nanotechnology. Spurred by studies of natural systems derived from molecular components such as lipids and enzymes that have evolved specific function from their 3D architecture, the goal of creating function through the assembly of simple precursors is an attractive pursuit. Natural proteins are a prime example of the wide array of functions that come about from the structural constraints imparted by relatively simple building blocks of amino acids and their respective side chains. Supramolecular materials derived from monomeric units that develop a function as a result of their aggregation are beginning to transition into neighboring fields spanning molecular devices and materials used for tissue engineering [1,2]. Development of new supramolecular assembly paradigms is complex, because the properties of the resulting materials need to be incorporated into the molecular design of the monomer, and those properties need to propagate into the assembled materials. Rational design of aggregate size and shape are also difficult to address given the complexity of hierarchical assembly and the need to balance the energetic parameters necessary for the desired aggregate structure to form [3]. Organic electronic materials are one subset of materials that may benefit from the order that supramolecular systems can provide [4]. In conjugated polymers, intramolecular delocalization is typically limited by the effective conjugation length of the material, and intermolecular interactions become increasingly important when

---

\**Pure Appl. Chem.* **84**, 861–1112 (2012). A collection of invited papers based on presentations at the 14<sup>th</sup> International Symposium on Novel Aromatic Compounds (ISNA-14), Eugene, OR, USA, 24–29 July 2011.

‡Corresponding author

considering macroscopic electronic transport processes [5]. The molecular approach of supramolecular chemistry can aid in the understanding of these intermolecular interactions by having discrete monomer sizes and rational control of the assembly.

## SUPRAMOLECULAR MATERIALS TOWARD BIOELECTRONIC APPLICATIONS

Rational design of supramolecular systems for organic electronic applications has become increasingly recognized as a viable route to functional materials [6–8]. We recently devised new supramolecular materials to fill a void in the field of bioelectronics. The design of our system was to bring gellators containing  $\pi$ -conjugated subunits into the aqueous phase for potential use in biological applications. We are motivated by past efforts to achieve organogelation of  $\pi$ -conjugated supramolecular structures and for the desire to prepare cellular scaffolds that incorporate electronic functionality. Our materials utilize the peptide/amide-based hydrogen bonding found in natural oligopeptides and proteins but with a  $\pi$ -conjugated subunit embedded directly into the peptide backbone [9–11]. This would provide a material that had a biologically relevant presentation of peptides for cellular environments and a core of  $\pi$ -conjugated functionality. We also hope that the versatility found in recent work of oligopeptide-based chromophore assembly can be used to more generally probe intermolecular interactions and their effect on energy delocalization within amyloid-like electronic materials [12,13].

### Synthetic strategy for rapid development of $\pi$ -conjugated peptide constructs

Our initial work to incorporate  $\pi$ -conjugated subunits directly into peptide backbones utilized the techniques developed for standard solid-phase peptide synthesis (SPPS) [14,15]. To accomplish this, a series of  $\pi$ -conjugated “amino acids” needed to be synthesized. This typically required lengthy synthetic routes often hindered by severe insolubilities. Although synthesizing the  $\pi$ -conjugated Fmoc protected “amino acids” to follow SPPS protocols was successful for the cases of bithiophene or stilbene, this strategy proved to be difficult for longer  $\pi$ -conjugated systems [9]. To overcome these limitations, we developed a simple procedure that required symmetric  $\pi$ -conjugated diacids [10]. The standard protocol for SPPS is to extend the peptide chain by reacting with a resin-bound N-terminal amine, so we sought out symmetric diacid  $\pi$ -conjugated subunits. It was envisioned that through proper activation of the diacid, cross-linking of two growing peptide chains on the solid-supported resin with a double amidation could be accomplished. Cleavage of the peptide from the resin would then yield a  $\pi$ -conjugated subunit flanked by two symmetrical peptide chains (Fig. 1).

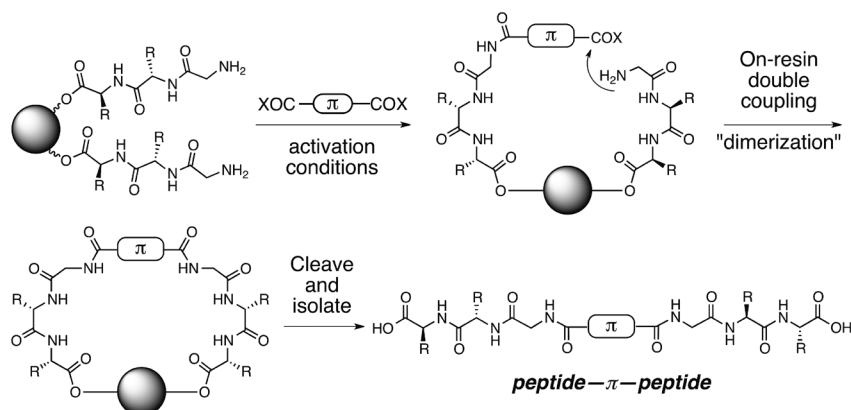


**Fig. 1** On-resin cross-linking of immobilized peptide chains via amidation of doubly activated  $\pi$ -conjugated diacids.

Conditions were screened for appropriate activation of the carboxylic acids and solvent conditions that would provide solubility of the  $\pi$ -conjugated diacid and proper swelling of the solid support resin. Symmetric diacids and dianhydrides representing broadly used p- and n-type semiconductors as well as strongly absorbing chromophores were readily synthesized (or commercially available) and successful dimerization on-resin to afford the desired peptide- $\pi$ -peptide monomers proceeded rapidly. This method was generally applicable to several diacids and dianhydrides, and the identity of the amino acid at the resin-bound peptide terminus involved in the coupling did not seem to influence the reaction. A typical procedure involves treating the resin with 0.3 equiv of diacid and 0.6 equiv of a proper activator followed by a second round of treatment with 0.2 equiv diacid and 0.4 equiv activator. We found that phosphonium coupling reagents (i.e., PyBOP) typically resulted in higher yields and fewer side reactions compared to typical uranium-based activators (i.e., HBTU), which formed appreciable amounts of tetramethylguanidinium capped N-terminal peptides arising when the uranium coupling reagent reacts directly with the N-terminal amine of the resin [16]. The two-step coupling conditions allowed for complete solubility of the diacid, as well as less monocoupled product where only one acid on the  $\pi$ -conjugated subunit underwent peptide amidation, and these conditions worked for a variety of differing amino acid sequences such as those shown with an oligophenylene vinylene (OPV) chromophore (Fig. 2). The yields of the couplings were modest (30–45 %) yet given the availability and opportunity costs of both the resin and diacids, this route provided a rapid and attractive means to the desired peptide- $\pi$ -peptide constructs.

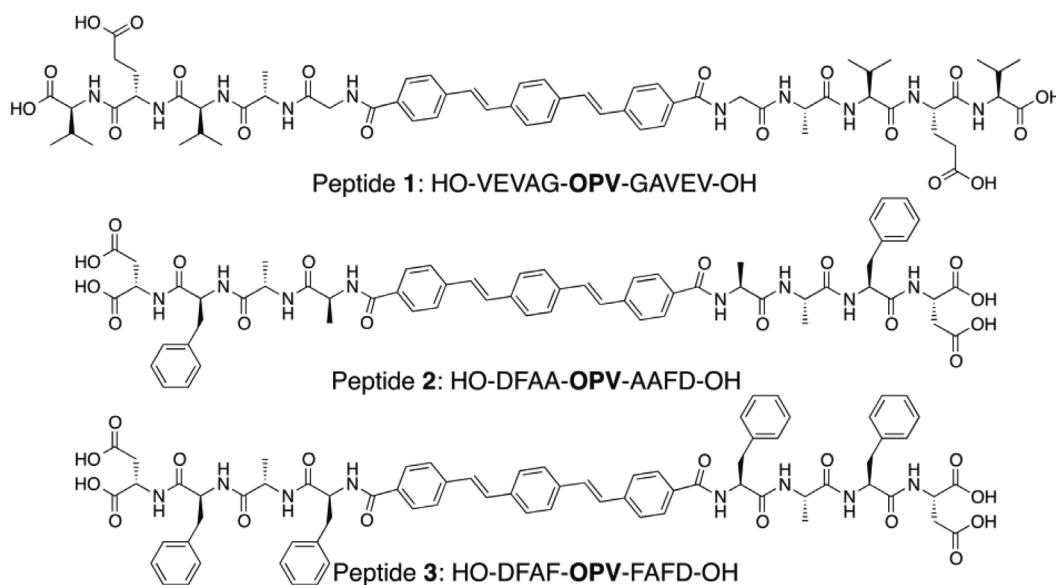


**Fig. 2** A series of peptide- $\pi$ -peptide conjugates containing an OPV subunit prepared via on-resin dimerization.

The peptides we prepared were designed to assemble with an appropriate pH trigger where the primary amino acid sequence contained enough ionizable groups to allow for aqueous solubility and enough Coulombic repulsion to hinder the assembly process in a specific pH range. Initial designs employed the use of the carboxylic acid side chains (aspartic and glutamic acids) allowing for negatively charged and soluble peptides in neutral or basic water. These peptides showed no signs of aggregation at basic pH either macroscopically or spectroscopically, with UV and photoluminescence spectra closely matching that of the corresponding OPV diacid monomer and no appreciable low-energy signal in the circular dichroism (CD) spectra. These peptides could then be triggered to assemble by

lowering the pH, effectively screening the Coulombic repulsion between the carboxylate residues by formal protonation to allow for favorable hydrogen-bonding networks to form (Figs. 3a,c). At low peptide weight percents (0.1–1.5 wt %), self-supporting hydrogels formed upon lowering the pH, and atomic force microscopy showed the formation of 1D nanostructures (Fig. 3b). The structures formed had dimensions of approximately 3–5 nm and lengths of microns, putting them into a size regime for soft organic electronic materials smaller than achievable routinely with typical nanolithography techniques and larger than what bottom-up molecular synthesis can provide.

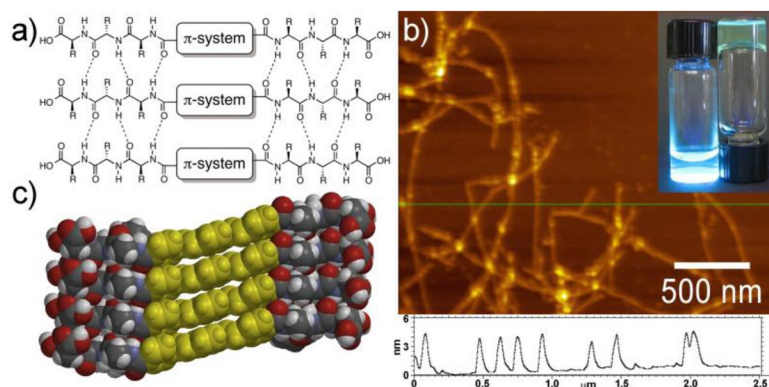


**Fig. 3** Illustration of the parallel  $\beta$ -sheet network within an aggregate (a). AFM of peptide **1** showing 1D nanostructures (b). The inset shows a molecularly dissolved aqueous peptide solution of **1** (left) and the hydrogel formed after assembly (right). Space-filling illustrations of the  $\pi$ -stacking and hydrogen-bond formation via self-assembly of **1** (c) [10].

The embedded  $\pi$ -conjugated subunits within the peptide backbones provided unique spectroscopic handles to probe the assembled structures (Fig. 4). Steady-state absorption and photoluminescence data for the assembled structures showed trends typically associated with H-like aggregates such as blue-shifted absorption and quenched red-shifted photoluminescence upon aggregation. CD for basic solutions showed little to no absorbance corresponding to the  $\pi$ -conjugated unit, but upon acidification and subsequent assembly, large induced CD signals showing bisignate Cotton effects were observed in the low-energy region of the spectra (250–600 nm), indicative of the subunit being held within a chiral environment. The steady-state spectroscopy indicates intimate  $\pi$ -conjugated subunit interactions within chiral aggregate structures.

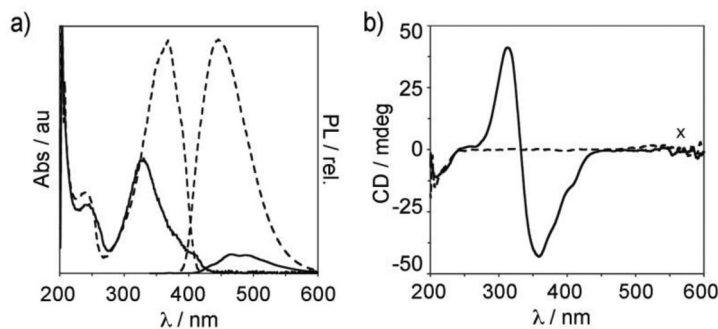


**Fig. 4** UV-vis and photoluminescence spectra (a) and CD spectra (b) of peptide **1** in its molecularly dissolved (basic pH, dashed line) and self-assembled (acidic pH, solid line) states. The X in (b) indicates unavoidable scattering at the spectroscopic concentrations required for measurement [10].

This spectroscopic handle is unique to peptide materials and provides the ability to probe differing assemblies within the peptide  $\pi$ -conjugated aggregates.  $\pi$ -Conjugated organogelators have been extensively studied to probe  $\pi$ - $\pi$  interactions and energy delocalization for organic electronic applications [17–21], and hydrogelators have been shown to be potentially useful scaffolds for many biotechnological applications [22,23]. The system developed here with the  $\pi$ -conjugated embedded directly into the peptide backbone provides a unique way to merge these two fields. We are currently exploring time-resolved spectroscopic properties of these assemblies as well as the impact that peptide structures have upon these properties.

### Alignment of supramolecular nanostructures

These peptides self-assemble into hydrogels whereby the component 1D nanostructures contain no long-range order. Alignment of these nanostructures could allow for even greater energy delocalization as well as aid the extension into bioelectronic materials and devices. We envisioned that the buried  $\pi$ -conjugated segments within the peptide nanostructures could facilitate energy migration, and having an aligned network could potentially increase the resulting charge/exciton migration length in the resulting materials. Recent work by Stupp and co-workers showcased a solution-based process to prepare aligned macrostructures of self-assembling peptide amphiphiles [24]. We recently reported that this solution extrusion achieved the alignment of hydrogen-bonding 1D nanostructures derived from peptide motifs bearing different  $\pi$ -conjugated subunits [11]. The shear forces present as the peptide solution is drawn from a syringe leads to a macroscopic material comprised of aligned nanostructures. These materials showed aligned domains over various length scales from the nanometer regime observed with SEM to the centimeter regime observed with polarized optical microscopy (Fig. 5).

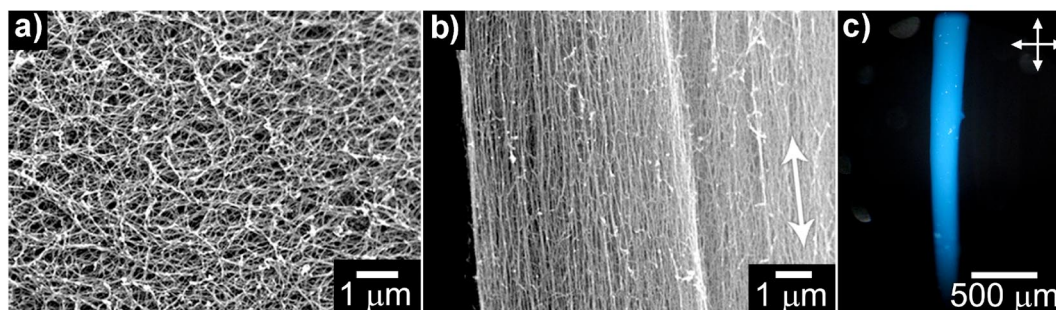


**Fig. 5** SEM images of an assembled random hydrogel of peptide **1** (a) and a hydrogel prepared using the shear-flow technique giving rise to aligned domains (b). Optical birefringence of the macroscale peptide hydrogel prepared using shear-flow as seen under crossed polarizers [11].

### Investigation of anisotropic photophysical and anisotropic electrical responses

The differences arising from macroscale alignment of the  $\pi$ -conjugated embedded peptide nanostructures were revealed through photophysical measurements on hydrogels composed of random and aligned nanostructures. Utilizing the shear-flow assembly technique to give aligned domains of supramolecular nanostructures gave spectroscopic signatures different from both monomer and randomly aligned samples. Both random and aligned hydrogels were assembled with relatively similar kinetics, (both with a rapid mixing of the peptide with an acidic medium) yet the alignment gave rise to differences in the nature of the electronic states of the supramolecular aggregate. From viewing a one-photon excited fluorescent image of an aligned sample, which also contains some randomly aligned hydrogel in the same field of view; one can observe the differences in the emission by changing the

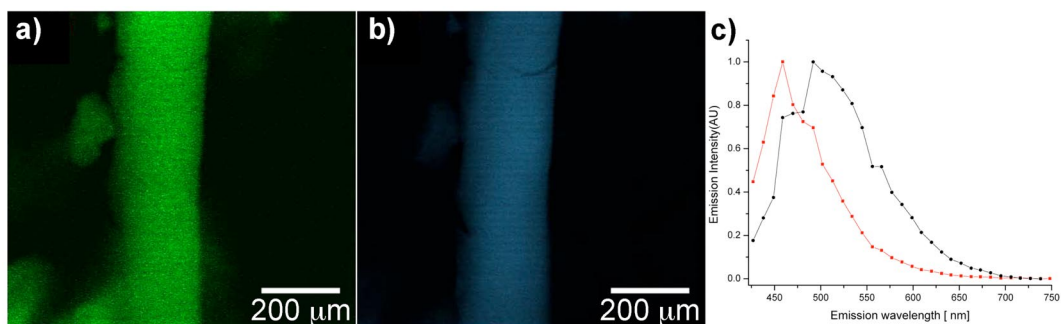


**Fig. 6** One-photon fluorescence images ( $\lambda_{\text{exc}} = 405 \text{ nm}$ ) of peptide **1** including both random hydrogel (diffuse spots) and aligned shear-flow produced sample. Emission was recorded through bandpasses set at  $530 \pm 20 \text{ nm}$  (a) and  $450 \pm 30 \text{ nm}$  (b). Normalized emission spectrum of random hydrogel (black) and aligned sample (red) (c).

spectral bandwidth used for the emission channel (Fig. 6). The low-energy green emission channel ( $530 \pm 20 \text{ nm}$  band pass) showed emission from both  $\pi$ -conjugated subunits of the aligned and random sample. Tuning the emission band pass filters to higher energy ( $450 \pm 30 \text{ nm}$ ) gave rise to emission predominately from the aligned sample.

There is still much to be learned about the nature of the emissive state and the differences between the aligned and random macrostructures. Since both aggregates are comprised of  $\pi$ -stacks in 1D nanostructures, it is reasonable to expect that the energetics of the emissive states would be similar for both the aligned and random macrostructures. The sharper higher-energy bands seen for the aligned macrostructures suggest that some electronic order is being introduced. The exact origin of this is still under investigation, yet it is speculated that the ordered aligned domains create a system that differs in the density or types of aggregates formed within the aligned material. The fact that the aligned macrostructure gave rise to emission from both channels seems to imply that the structure as a whole is comprised of both aligned and unaligned domains. With the spectroscopic signatures suggesting electronic order we sought to investigate the effect this order had on the orientation and gate-field-dependent conductances of an aligned sample of quaterthiophene peptide nanostructures. It was found that the mobility measured within the aligned sample was anisotropic, with an order of magnitude increase in the mobility when measured parallel to the direction of the aligned nanostructures ( $0.03 \pm 0.005 \text{ cm}^2 \text{ V}^{-1} \text{ s}^{-1}$ ) vs. the measurements taken running perpendicular to the alignment ( $0.0014 \pm 0.0001 \text{ cm}^2 \text{ V}^{-1} \text{ s}^{-1}$ ) [11].

These nanostructures offer a unique perspective on bioelectronic materials with  $\pi$ - $\pi$  interactions prepared via aqueous self-assembly as a means of studying interactions between  $\pi$ -conjugated subunits and their resulting properties. We have demonstrated synthetic methodologies that afford a generic template for aqueous self-assembling systems that contain an embedded  $\pi$ -conjugated subunit from a simple on-resin synthesis. We have also shown the ability to go beyond that of fundamental study of  $\pi$ -conjugated aggregates with the demonstration of a working device, by forming electrical contacts to an aqueously assembled system to obtain measureable field-effect mobilities. The technically simple fabrication method of shear-flow assembly leading to the development of aligned domains also allows for the study of systems with anisotropic mobilities. This versatile system of peptide- $\pi$ -peptide constructs can now be used to study  $\pi$ - $\pi$  interactions in the photophysical and device regimes. Current work involves obtaining a better understanding of the spectroscopic differences seen with the aligned fibrous domains vs. the random networks formed in bulk hydrogels. More elaborate spectroscopy is being done to tease out the differing emission characteristics observed in the aligned and the random samples to determine if the higher-energy emission bands from the aligned noodle sample are due to electronic “order” and the minimization of low-lying trap sites, or due to some other mechanism. Structural analogs of these peptides are also being created to study the interchromophore interactions

more closely. We hope to use this versatile system for the fundamental understanding of  $\pi$ - $\pi$  interactions within biologically relevant nanostructures and better rationalize how order and orientation affect the properties of these functional supramolecular materials.

## ACKNOWLEDGMENTS

Generous financial support was provided by Johns Hopkins University and the Department of Energy, Office of Basic Energy Sciences (DE-SC0004857 peptide nanomaterials synthesis). B.W. was supported by the Harry and Cleio Greer Fellowship (JHU).

## REFERENCES

1. S. I. Stupp. *Chem. Rev.* **105**, 1023 (2005).
2. R. V. Ulijn, D. N. Woolfson. *Chem. Soc. Rev.* **39**, 3349 (2010).
3. J. M. Zayed, N. Nouvel, U. Rauwald, O. A. Scherman. *Chem. Soc. Rev.* **39**, 2806 (2010).
4. F. J. M. Hoeben, P. Jonkheijm, E. W. Meijer, A. P. H. J. Schenning. *Chem. Rev.* **105**, 1491 (2005).
5. J. Cornil, D. A. dos Santos, X. Crispin, R. Silbey, J. L. Brédas. *J. Am. Chem. Soc.* **120**, 1289 (1998).
6. D. González-Rodríguez, A. P. H. J. Schenning. *Chem. Mater.* **23**, 310 (2011).
7. A. P. H. J. Schenning, E. W. Meijer. *Chem. Commun.* **41**, 3245 (2005).
8. J. D. Tovar, S. R. Diegelmann, B. D. Wall. In *Nanoelectronics: Nanowires, Molecular Electronics, and Nanodevices*, 1<sup>st</sup> ed., K. Iniewski (Ed.), pp. 289–318, McGraw-Hill, New York (2010).
9. S. R. Diegelmann, J. M. Gorham, J. D. Tovar. *J. Am. Chem. Soc.* **130**, 13840 (2008).
10. G. S. Vadehra, B. D. Wall, S. R. Diegelmann, J. D. Tovar. *Chem. Commun.* **46**, 3947 (2010).
11. B. D. Wall, S. R. Diegelmann, S. Zhang, T. J. Dawidczyk, W. L. Wilson, H. E. Katz, H.-Q. Mao, J. D. Tovar. *Adv. Mater.* **23**, 5009 (2011).
12. E. K. Schillinger, E. Mena-Osteritz, J. Hentschel, H. G. Börner, P. Bäuerle. *Adv. Mater.* **21**, 1562 (2009).
13. D. A. Stone, L. Hsu, S. I. Stupp. *Soft Matter* **5**, 1990 (2009).
14. R. B. Merrifield. *J. Am. Chem. Soc.* **85**, 2149 (1963).
15. G. B. Fields, R. L. Noble. *Int. J. Pept. Protein Res.* **35**, 161 (1990).
16. H. Gausepohl, U. Pielers, R. W. Frank. *Peptides: Chemistry and Biology*, J. A. Smith, J. E. Rivers (Eds.), ESCOM, Leiden, **524**, 523 (1992).
17. A. Ajayaghosh, V. K. Praveen. *Acc. Chem. Res.* **40**, 644 (2007).
18. A. Ajayaghosh, V. K. Praveen, C. Vijayakumar. *Chem. Soc. Rev.* **37**, 109 (2008).
19. X. Q. Li, V. Stepanenko, Z. J. Chen, P. Prins, L. D. A. Siebbeles, F. Würthner. *Chem. Commun.* 3871 (2006).
20. S. Prasanthkumar, A. Saeki, S. Seki, A. Ajayaghosh. *J. Am. Chem. Soc.* **132**, 8866 (2010).
21. S. Prasanthkumar, A. Gopal, A. Ajayaghosh. *J. Am. Chem. Soc.* **132**, 13206 (2010).
22. G. A. Silva, C. Czeisler, K. L. Niece, E. Beniash, D. A. Harrington, J. A. Kessler, S. I. Stupp. *Science* **303**, 1352 (2004).
23. J. P. Schneider, D. P. Pochan, B. Ozbas, K. Rajagopal, L. Pakstis, J. Kretsinger. *J. Am. Chem. Soc.* **124**, 15030 (2002).
24. S. M. Zhang, M. A. Greenfield, A. Mata, L. C. Palmer, R. Bitton, J. R. Mantei, C. Aparicio, M. O. de la Cruz, S. I. Stupp. *Nat. Mater.* **9**, 594 (2010).